Drug Design, Development and Therapy

Dovepress
open access to scientific and medical research

Open Access Full Text Article

ORIGINAL RESEARCH

miR-346 Inhibited Apoptosis Against Myocardial Ischemia-Reperfusion Injury via Targeting Bax in Rats

This article was published in the following Dove Press journal:
Drug Design, Development and Therapy

Xiangwei Lv[1,*]
Pan Lu[1,*]
Yisen Hu[2]
Tongtong Xu[1]

[1]Department of Cardiology, Affiliated Hospital of Guilin Medical University, Guilin 541001, Guangxi Zhuang Autonomous Region, People's Republic of China; [2]Department of Cardiology, First Affiliated Hospital of Guangxi Medical University, Nanning 530021, Guangxi Zhuang Autonomous Region, People's Republic of China

*These authors contributed equally to this work

Purpose: Myocardial ischemia-reperfusion injury (MIRI) is a common pathophysiological process after occlusion of the blood vessels to restore blood supply. Apoptosis is one of the ways of myocardial cell death in this process. MicroRNAs (miRNAs), a class of short and noncoding RNAs, are involved in multiple biological processes by post-transcriptionally targeting their downstream effectors. To date, whether miRNAs exert biological effects in myocardial ischemia-reperfusion (I/R) injury remains to be further studied.

Methods: In this study, we induced MIRI model by ligating rat left anterior descending artery (LAD) for 30 mins and reperfusion for 2 hrs. The differential expression profile of miRNAs in rat models of MIRI was analyzed by miRNAs sequencing.

Results: We found that miRNAs sequencing analysis showed the expressions of 15 types of miRNAs, including miR-346, were downregulated and 29 types of miRNAs were elevated in the MIRI rat model. We observed the key regulator of apoptosis Bax was a predicted downstream target of miR-346 using online software TargetScan. And luciferase reporter assay was utilized to certify this prediction. Over-expression of miR-346 can attenuate myocardial injury and narrow infarct area by inhibiting myocardial cell apoptosis in rat models.

Conclusion: This study revealed a novel pathway, miR-346/Bax axis, in the regulation of apoptosis in MIRI and which might be a new molecular mechanism and therapeutic target.

Keywords: miR-346, myocardial ischemia-reperfusion injury, apoptosis, Bax

Introduction

Acute myocardial infarction (AMI) is the leading cause of death and disability worldwide. Thrombolysis and intervention are the main reperfusion therapy strategies, often accompanied by myocardial ischemia-reperfusion injury (MIRI).[1–6] MIRI is myocardial damage or dysfunction after blood flow is restored after the blood supply to the heart patient is interrupted, which could cause cardiomyocyte apoptosis, pyroptosis, ferroptosis and necrosis, and even cardiac arrest.[4,7,8] Studies have confirmed that apoptosis plays an indispensable role in the initiation and progression of MIRI.[9–11] Currently, many experimental and clinical studies have confirmed that ischemia-reperfusion (I/R) induced cardiac injury is related to various microRNAs (miRNAs) and some mechanisms have been reported under specific experimental conditions.[12–14] However, those findings for clinical application are not enough, and detail mechanisms of MIRI still need to be further studied.

MiRNAs are small, endogenous, non-coding RNAs subgroup containing 18 to 23 nucleotides.[15,16] Typically, miRNAs silence their mRNA target through binding to

Correspondence: Tongtong Xu
Department of Cardiology, Affiliated Hospital of Guilin Medical University, Guilin 541001, Guangxi Zhuang Autonomous Region, People's Republic of China
Tel +86 773-2807731
Email xutongtongguilin@glmc.edu.cn

submit your manuscript | www.dovepress.com
DovePress
http://doi.org/10.2147/DDDT.S245193

complementary recognition sequences of mRNA and inhibiting its expression.[17,18] In past decades, it has been proved that miRNA acts as a regulator in different biological processes, such as cardiogenesis, tumorigenesis, cell differentiation and apoptosis.[19,20] miR-346 is positioned in the second intron of the glutamate receptor ionotropic delta 1 (GRID1) gene, which was firstly identified to be redundant in follicular thyroid carcinoma (FTC).[21–23] Several studies have showed that miR-346 regulates many pathological events, including cell differentiation, carcinogenesis and inflammatory response.[23–28] Nevertheless, the function of miR-346 in MIRI remains unclear.

In this experiment, we explored potential molecular regulatory mechanisms by establishing a MIRI rat model. MicroRNA sequencing analysis displayed the expression of miR-346, one of the 15 downregulated genes, was dramatically decreased in the model. Subsequently, miR-346 was predicted to be an upstream regulatory factor of Bax gene, a crucial regulator for cell apoptosis,[29–31] using bioinformatic website TargetScan (http://www.targetscan.org/). We then used a luciferase reporter assay to confirm this prediction. Furthermore, over-expression of miR-346 could sufficiently attenuate MIRI and narrow infarct area by inhibiting myocardial cell apoptosis in a rat model. In the present study, we investigated that over-expression of miR-346 inhibits cardiomyocyte apoptosis and attenuates MIRI in rats by targeting Bax.

Materials and Methods

Animals and Ethics

Male Sprague-Dawley rats (200–250 g) were raised in Guangxi Medical University Experimental Animal Center (SYXK [Gui] 2014–0003). All animals are treated with the Guiding Opinions on the Treatment of Laboratory Animals issued and the Laboratory Animal-Guideline for Ethical Review of Animal Welfare issued by the National Standard GB/T35892-2018 of the People's Republic of China. All operations in animal experiments are performed under anesthesia to avoid pain and suffering.

MIRI Rat Model Construction

We anesthetized rats using pentobarbital sodium at a dosage of 40 mg/kg before tracheal intubation. The left anterior descending artery (LAD) was ligated for 30 min and then reperfused for 120 min. After reperfusion, we separated the heart under anesthesia. Pseudo-surgical animals perform the same operation without blocking LAD. When the ST segment of the 12-lead ECG is significantly elevated and the ligated blood supply area appears pale or gray, it represents the success of ischemia. Subsequently, the ligature was released, the ST segment descended and the arrhythmia appeared, indicating successful reperfusion.

Total RNA Extraction and miRNA Sequencing

According to the random principle, six rats were divided into Sham group and I/R group. Total RNA extraction was performed using the miRNeasy Micro Kit (Qiagen, Germany). Quality testing by Bioanalyzer 4200 (Agilent, USA). The next-generation libraries were prepared using VAHTS mRNA-seq v2 Library Prep Kit for Illumina® (Vazyme, China). Library quality was determined by Bioanalyzer 4200 (Agilent, USA). Then RNA-seq libraries were sequenced in the HiSeq X10 system (Illumina, USA) on a 150 bp paired-end run according to the protocols of the manufacturer.

RT-PCR Assay

Total RNA and miRNA were extracted using the RNAeasy Mini Kit (Qiagen, Netherlands) and the miRcute miRNA isolation kit (TIANGEN Biotech, China) according to the protocols of the manufacturer. Quantitative detection of total RNA and miRNA was determined by a NanoDrop 2000 spectrophotometer (Thermo Scientific, USA). The miR-346 level detection and RNA reverse transcription to cDNA were performed utilizing the miRcute Plus miRNA First Strand cDNA Synthesis Kit (TIANGEN Biotech, China) according to the manufacturer's instructions. Primers for miR-346 and U6 in this study were designed and synthesized by TaKaRa (Kyoto, Japan) (Table 1).

Table 1 Primers Used for RT-PCR

Primer/Probe	Sequences
miR-346	F: 5′-ACACTCCAGCTGGGTGTCTGCCTGAGTGCCT-3′ R: 5′-CTCAACTGGTGTCGTGGAGTCGGCAATTCAGTTGAGAGAGGCAG-3′
U6	F: 5′CTCGCTTCGGCAGCACA-3′ R: 5′AACGCTTCACGAATTTGCGT-3′

RT-PCR detection of miR-346 was performed using an ABI 7500 real-time PCR system (Applied Biosystems, CA, USA) according to the protocols of the manufacturer. The fold change of miR-346 was calculated using the $2^{-\Delta\Delta Ct}$ method, and U6 was used as an internal control.

Luciferase Reporter Assay

5×10^4 HEK293T cells in each well were plated into a 24-well plate. The Bax luciferase reporter with binding sites for miR-346 was synthesized and subcloned into pGL3-Control Vector (Promega, Madison). Lipofectamine 2000 (Invitrogen) was used to transfect the luciferase reporter with wild type (WT) or mutant type (MT) miR-346-mimics (GenePharma, Shanghai China) according to the protocols of the manufacturer. After 48 hrs of transfection, luciferase activity was analyzed by dual luciferase reporting kit (Promega), which was measured by a SpectraMax L (Molecular Devices, CA, USA).

Adeno-Associated Virus Transfection and Experimental Animal Grouping

Recombinant adeno-associated virus (AAV, 2×10^{11} vector genomes (vg) particles/per rat) was designed and constructed by Hanbio Biotechnology (Shanghai, China), AAV-miR-346 over-expressed miR-346, AAV-miR-346-antago low-expression miR-346. AAV-NC served as a negative control group. Thirty rats were divided into five groups depending on the random principle, with six rats in each group, including the Sham, I/R, AAV-NC, AAV-miR-346 and AAV-miR-346-antago groups. After 2 weeks of injection of AAV through the tail vein, we anesthetized rats and performed experiments.

HE and TTC Detection

The myocardial tissues were collected and then fixed with 4% paraformaldehyde for 24 h in accordance with the standard procedures. Three millimeter-thick myocardial sections were embedded in paraffin. Hematoxylin and eosin (HE) test subsequently perform. The optical microscope (CKX41, Olympus, Tokyo, Japan) at × 400 was used to visualize the degree of heart damage and capture them into a photograph. MIRI was scored according to the histomorphological criteria.[32] TTC staining was carried out to measure the myocardial infarct size. Briefly, after reperfusion for 120 mins, we harvested the heart immediately and maintained it at −80°C until use. Then, the heart was sliced into 5 mm-thick sections and subsequently incubated with 3% TTC for 30 mins at 37°C. Red represents the non-infarct area, and gray and white represent the infarct area. Image-Pro Plus 6.0 software was used to evaluate the infarct area.

ELISA Measurement

After the reperfusion, we collected the whole blood specimens from blood circum. And then we centrifuged the bloods samples, immediately, at 12,000 g for 20 mins at 4°C. The collected supernatant was stored in a −20°C refrigerator for testing. A suite of commercial kits was used to test the level of serum cTnT in accordance with the manufacturer's instructions (Cusabio, China).

TUNEL Assay

TUNEL method with a detection kit (Roche, Germany) was used to estimate cell apoptosis in myocardial tissues following the manufacturer's protocol. The TUNEL-positive cells were identified by green nuclei, and blue represents normal nuclei. Each slice was randomly captured three visual fields. We used the following formula to calculate the apoptosis index (AI): AI = (number of positive cells/total number of cells) × 100%. The experimental data were analyzed using Image-Pro Plus 6.0 software.

Western Blot Analysis

Total protein was lysed in the RIPA buffer (Beyotime, China). BCA protein assay kit (Beyotime, China) was carried out to measure the protein concentration. After SDS-PAGE assay, we transferred the proteins onto PVDF membranes. Then, 5% non-fat milk was determined to block the membranes at room temperature for 2 h. We incubated the membranes with primary antibodies overnight at 4°C followed by washing 5 times using phosphate buffered saline supplemented with Tween 20 (PBST). Subsequently, secondary antibodies were incubated 2 h at room temperature. Finally, the protein bands on membranes were took into visualization using chemiluminescence system (Amersham Pharmacia). The primary and secondary antibodies used were listed below: Bcl-2 (1:500, Abcam), Bax (1:1000, CST), Cleaved Caspase-3 (1:1000, CST), GAPDH (1:1000, CST) and HRP (1:1000, Beyotime). We used GAPDH as the endogenous control in this assay. The gray value of each band was calculated by Image-Pro Plus 6.0 software.

Statistical Analysis

GraphPad Prism 5.0 software was used to perform all the data in this study. Data were displayed as the means ± SEM. Multiple comparisons were carried out by single-factor variance analysis. $P < 0.05$, there was statistical significance.

Results

Successful Establishment of the Rat I/R Model

ECG examination showed that the ST segment was significantly increased in 30 mins after ischemia, and the ST segment was decreased in 120 mins after reperfusion. At the same time, reperfusion arrhythmia appeared, which marked the successful establishment of rat I/R model (Figure 1).

Expression of miR-346 Was Decreased in Rat I/R Model

To elucidate the expression of miRNAs after I/R, we conducted a miRNA sequencing assay for Sham and I/R group. The heat-map results displayed the significant changes of miRNAs. We observed that the expressions of 15 miRNAs were downregulated and 29 miRNAs were upregulated in the I/R group by comparison to the Sham group, as showed in Figure 2A–C. Among the 15 downregulated miRNAs, we found miR-346 which had not been reported to participate in MIRI. Subsequently, we certified the expression of miR-346 using RT-PCR analysis, and found an obvious decrease in the I/R group rather than the Sham group (Figure 2D).

miR-346 Directly Inhibited the Transcription of Bax Gene

To explore the potential biological functions of miR-346, we used online bioinformatics software TargetScan (http://www.targetscan.org/) to predict the downstream targets of miR-346 in human and rat. After analysis, we found that the key regulator of apoptosis Bax contained the potential binding sites for miR-346 in its 3′ UTR (Figure 3A and B). To further verify the direct interaction between miR-346 and Bax gene, we constructed Bax luciferase reporter binding sites for miR-346 into pGL3 vector, respectively. Then, the Bax luciferase reporter was separately co-transfected with WT or MT miR-346 mimics into HEK293 cells. Luciferase assay revealed the relative luciferase activity in cells co-transfected with Bax luciferase reporter and WT miR-346 mimics was significantly decreased compared with MT miR-346 mimics and negative controls (NC) (Figure 3C). The outcomes strongly suggested miR-346 repressed the transcription of Bax through the binding site in its 3′UTR.

Over-Expression of miR-346 Attenuated MIRI

(1) We first used TTC staining to detect changes in myocardial infarct size in each group. As shown in Figure 4A and B, no

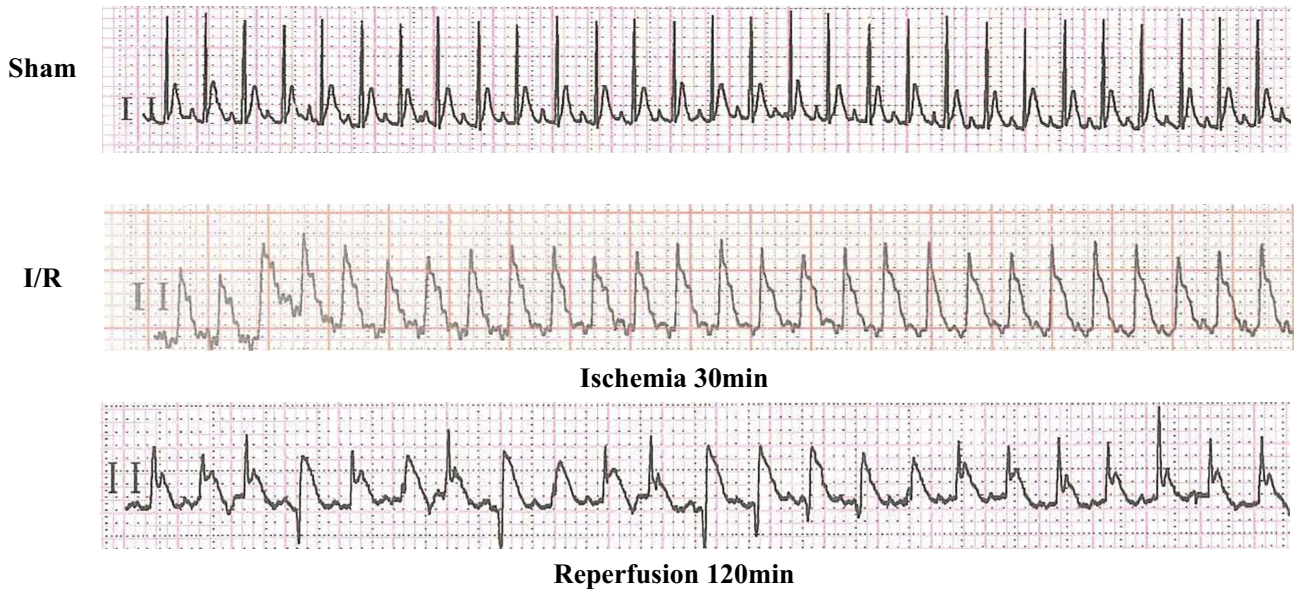

Figure 1 Changes in the ECG when the rat I/R model was established.

A

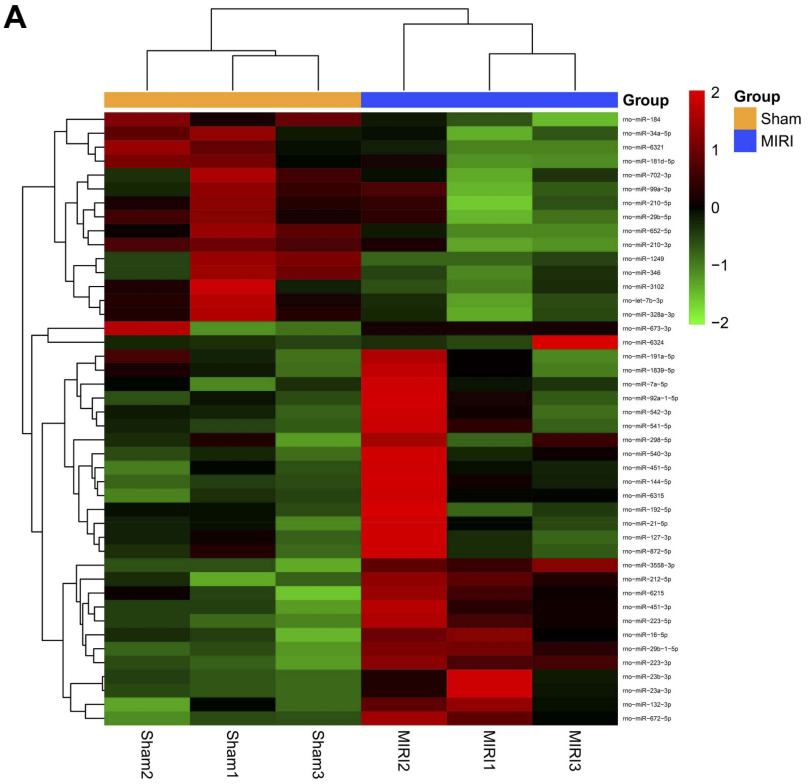

B

miRNA	Direction	*P* Value	False Discovery Rate
rno-miR-1249	down	0.014828633	0.234217
rno-miR-346	down	0.000648994	0.028312
rno-miR-652-5p	down	0.013725292	0.228101
rno-miR-6321	down	2.53052E-05	0.001766
rno-miR-184	down	0.009580758	0.189089
rno-miR-210-5p	down	0.026016809	0.313099
rno-let-7b-3p	down	0.006820113	0.158681
rno-miR-702-3p	down	0.017274891	0.241157
rno-miR-210-3p	down	0.000914188	0.02972
rno-miR-328a-3p	down	0.001629569	0.043748
rno-miR-3102	down	0.043614531	0.362416
rno-miR-181d-5p	down	0.002399057	0.059805
rno-miR-29b-5p	down	0.03889877	0.348094
rno-miR-34a-5p	down	0.036830732	0.348094
rno-miR-99a-3p	down	0.037285603	0.348094

C

miRNA	Direction	*P* Value	False Discovery Rate
rno-miR-192-5p	up	0.044796985	0.363585
rno-miR-127-3p	up	0.035697591	0.348094
rno-miR-542-3p	up	0.036702188	0.348094
rno-miR-872-5p	up	0.032673959	0.348094
rno-miR-191a-5p	up	0.043257109	0.362416
rno-miR-451-5p	up	0.012792584	0.223231
rno-miR-21-5p	up	0.009752458	0.189089
rno-miR-298-5p	up	0.018044756	0.242216
rno-miR-92a-1-5p	up	0.016106641	0.234217
rno-miR-7a-5p	up	0.034952932	0.348094
rno-miR-1839-5p	up	0.010488362	0.192655
rno-miR-132-3p	up	0.041088321	0.358496
rno-miR-16-5p	up	0.001428004	0.041531
rno-miR-144-5p	up	8.19016E-05	0.004764
rno-miR-672-5p	up	0.038394122	0.348094
rno-miR-6215	up	0.049848167	0.366609
rno-miR-451-3p	up	0.015680748	0.234217
rno-miR-673-3p	up	0.030084509	0.348094
rno-miR-6315	up	0.031022814	0.348094
rno-miR-541-5p	up	0.000936739	0.02972
rno-miR-223-5p	up	0.000915377	0.02972
rno-miR-212-5p	up	0.000289085	0.014413
rno-miR-29b-1-5p	up	9.42817E-06	0.001097
rno-miR-223-3p	up	2.8266E-06	0.000493
rno-miR-540-3p	up	0.023847323	0.29724
rno-miR-23b-3p	up	1.47131E-05	0.001284
rno-miR-23a-3p	up	2.47048E-06	0.000493
rno-miR-3558-3p	up	0.007760073	0.169267
rno-miR-6324	up	0.020921462	0.270429

D

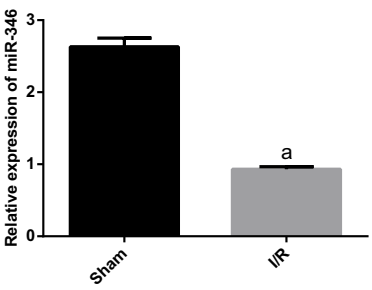

Figure 2 Downregulation of miR-346 in the I/R group. (**A**) Heat-map of sequencing data of miRNAs. Red and green color represent up- and down-regulation, respectively. (**B**) and (**C**) Tables for details of 15 downregulated genes and 29 upregulated genes. (**D**) RT-PCR assay for the expression of miR-346 (n=6). Note that $^{a}P < 0.05$ against the Sham group.

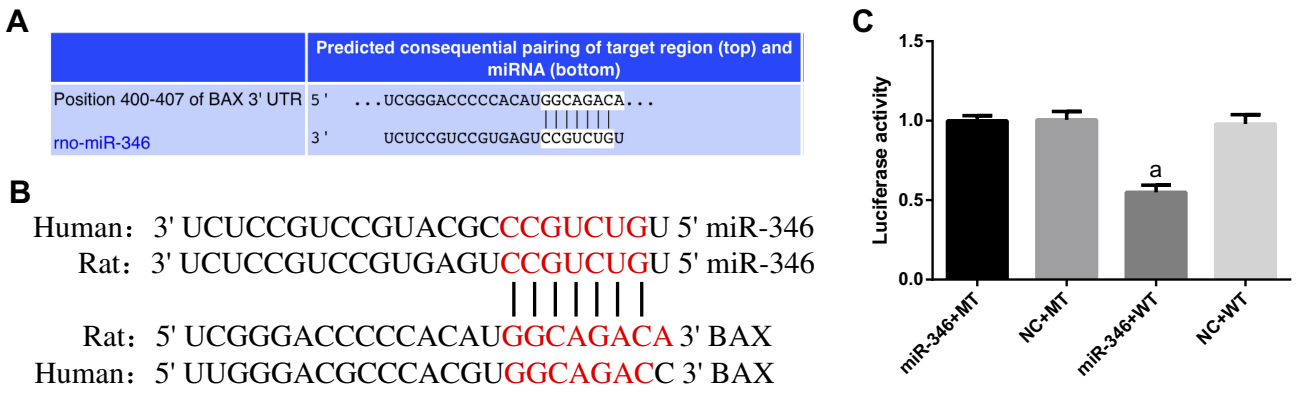

Figure 3 miR-346 directly repressed the expression of Bax gene. (**A**) Online software TargetScan revealed the predicted binding site of miR-346. (**B**) Complementary sequence between miR-346 and Bax in human and rat. (**C**) The effect of miR-346 on the luciferase activity was determined by luciferase reporter assays. miR-346 repressed the transcription of Bax gene. Note that $^{a}P < 0.05$ against the miR-346+MT group.

myocardial infarction was found in the Sham group, and the infarct size in the I/R group was enlarged. However, over-expression of miR-346 (AAV-miR-346 group) reduced infarct size by comparison to the I/R and AAV-NC group.

(2) Moreover, we further examined histopathological changes using HE, and also detected changes in the myocardial damage marker cTnT. Displayed in Figure 5A–C, the Sham group had a regular arrangement of myocardial structures, normal fibers, and no bleeding or necrosis. However, the I/R group found severe myocardial damage, including myocardial fibrosis, inflammatory cell infiltration, and cardiomyocyte edema, and serum cTnT levels were significantly elevated. Importantly, the degree of myocardial damage was reduced in the AAV-miR-346 group in comparison to the I/R and AAV-NC group, and we also observed a significant decrease in serum cTnT levels.

miR-346 Suppressed Cardiomyocyte Apoptosis via Targeting Bax Gene

(1) To figure out the cardiomyocyte apoptosis during MIRI, we utilized TUNEL staining to illustrate the apoptosis in the Sham, I/R, AAV-NC, AAV-miR-346 and AAV-miR-346-antago groups (Figure 6A and B). TUNEL staining displayed the apoptosis rate in the I/R group was higher than the Sham group; while in the AAV-miR-346 group, the apoptosis rate was lower than I/R and AAV-NC group.

(2) Furthermore, to clear the mechanisms of miR-346 in cell apoptosis during MIRI, we explored the protein

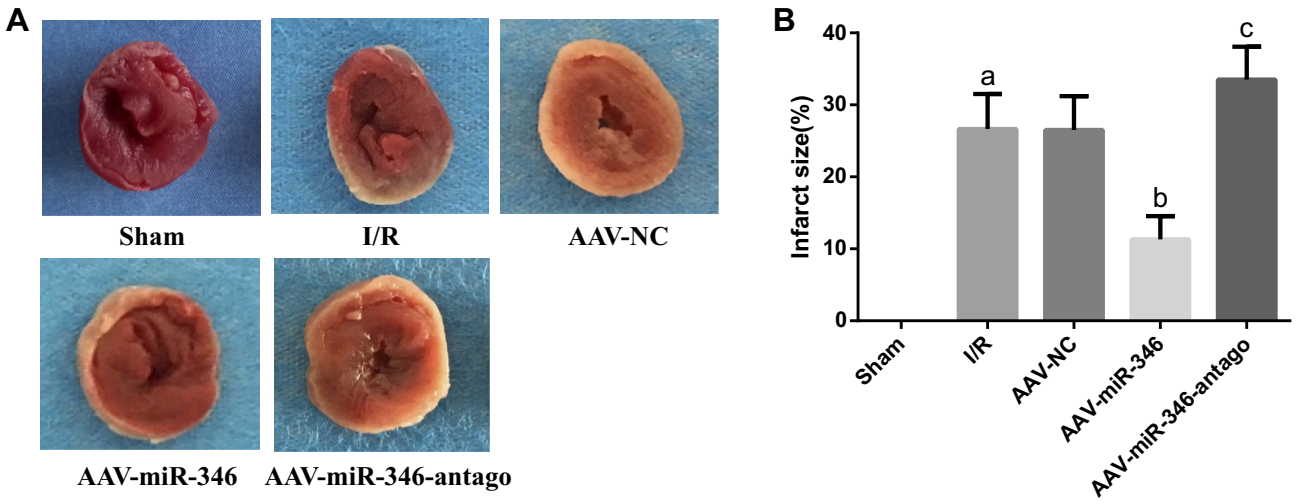

Figure 4 Over-expression of miR-346 can reduce myocardial infarct size. (**A**) TTC detection of Sham, I/R, AAV-NC, AAV-miR-346 and AAV-miR-346-antago groups. White and gray represent infarct areas and red represents non-infarct areas. (**B**) Infarct size scores. Note that $^{a}P < 0.05$ against the Sham group. $^{b}P < 0.05$ against the I/R group. $^{c}P < 0.05$ against the I/R or AAV-NC group.

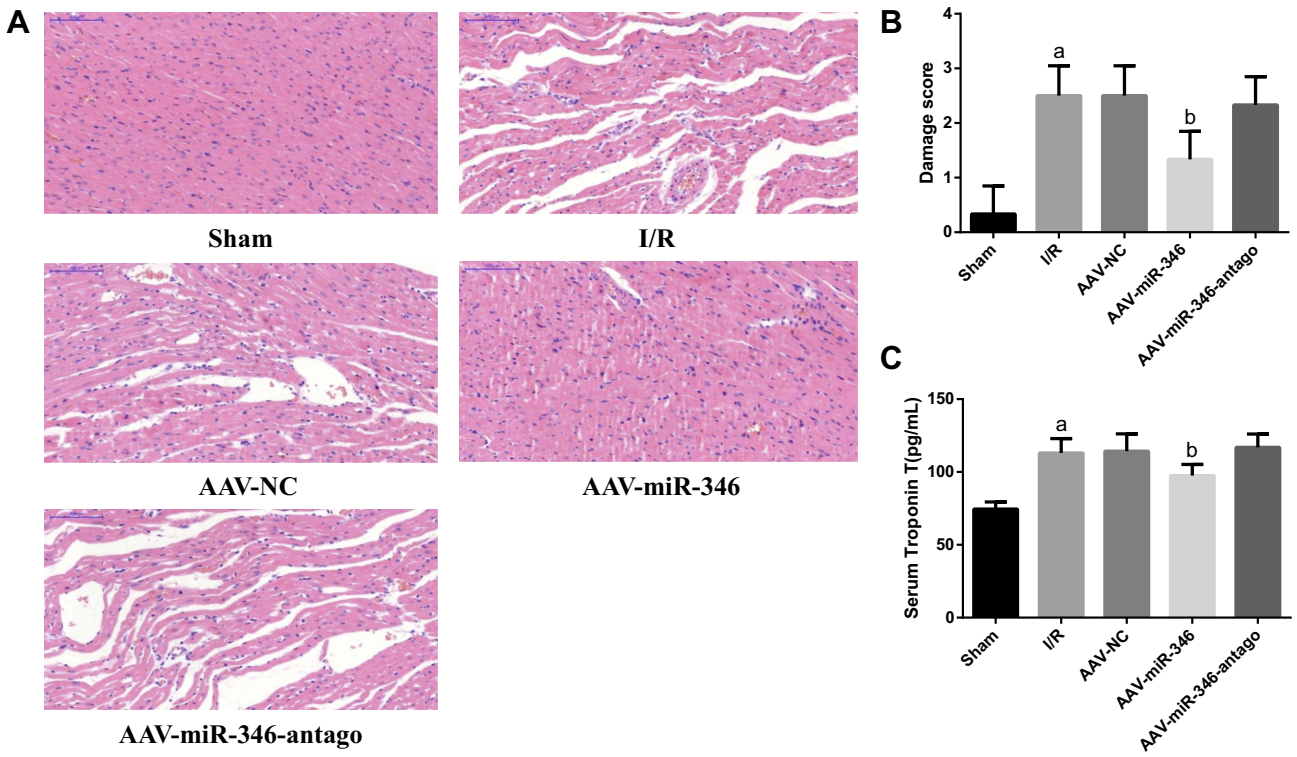

Figure 5 Over-expression of miR-346 attenuates histopathological changes and myocardial damage. (**A**) HE detection of Sham, I/R, AAV-NC, AAV-miR-346 and AAV-miR-346-antago groups (x200). (**B**) Myocardial injury scores. (**C**) Serum myocardial injury marker cTnT levels. Note that $^{a}P < 0.05$ against the Sham group. $^{b}P < 0.05$ against the I/R or AAV-NC group.

levels of Bcl-2, Bax, Cleaved Caspase-3 and Caspase-3, which were apoptosis related genes, using Western blotting assay (Figure 7A). The Bcl-2/Bax ratio was negatively correlated with cardiomyocyte apoptosis. We found in the experiment that the Bax protein expression increased and Bcl-2/Bax ratio in the I/R group decreased by comparison to the Sham group. However, over-expression of miR-346 significantly reduced Bax protein expression and increased the Bcl-2/Bax ratio compared to the I/R and AAV-NC group (Figure 7B and C). Meanwhile, the relative protein level of Cleaved Caspase-3/Caspase-3 ratio in the I/R group was notably higher than the Sham group; while in the AAV-miR-346 group, the relative protein level of Cleaved Caspase-3/Caspase-3 ratio was distinctly lower than I/R and AAV-NC group (Figure 7D). Those results clearly evidenced that miR-346 limited cell apoptosis against MIRI through regulating the expression of Bax gene.

Discussion

MIRI is a common pathophysiological event that there is temporally restricted blood supply to the heart and then restored back, while the damages to the tissues could not be recovered completely even worsening myocardial damage after reperfusion.[33,34] There are several biological processes related to myocardial damage, such as apoptosis, pyroptosis, ferroptosis, autophagy and necrosis of cardiomyocyte.[35–38] Generally, myocardial apoptosis mainly causes heart dysfunction and eventually lead to heart failure during MIRI.

MiRNAs, a large subgroup of non-coding RNAs, functionally regulate the transcriptional level of its target genes.[39–42] Increasing studies indicate miRNAs have been proved to be involved in I/R-induced cardiac injury.[8,12,20,43] Recently, several studies have demonstrated that miRNAs are related to cardiac events, including muscle contraction, heart growth and conductance of electric signal.[44–48] However, functions of miRNAs in MIRI still calling for further illustrated. Previous reports showed that miR-346 regulates many pathological events, including cell differentiation, carcinogenesis and inflammatory response.[21,23,24,26] Nevertheless, whether miR-346 exerts biological functions in MIRI are still little known.

In our study, the expression of miRNAs was analyzed by miRNA sequencing after the MIRI rat model establishment. Data shown that there were 44 differential miRNAs

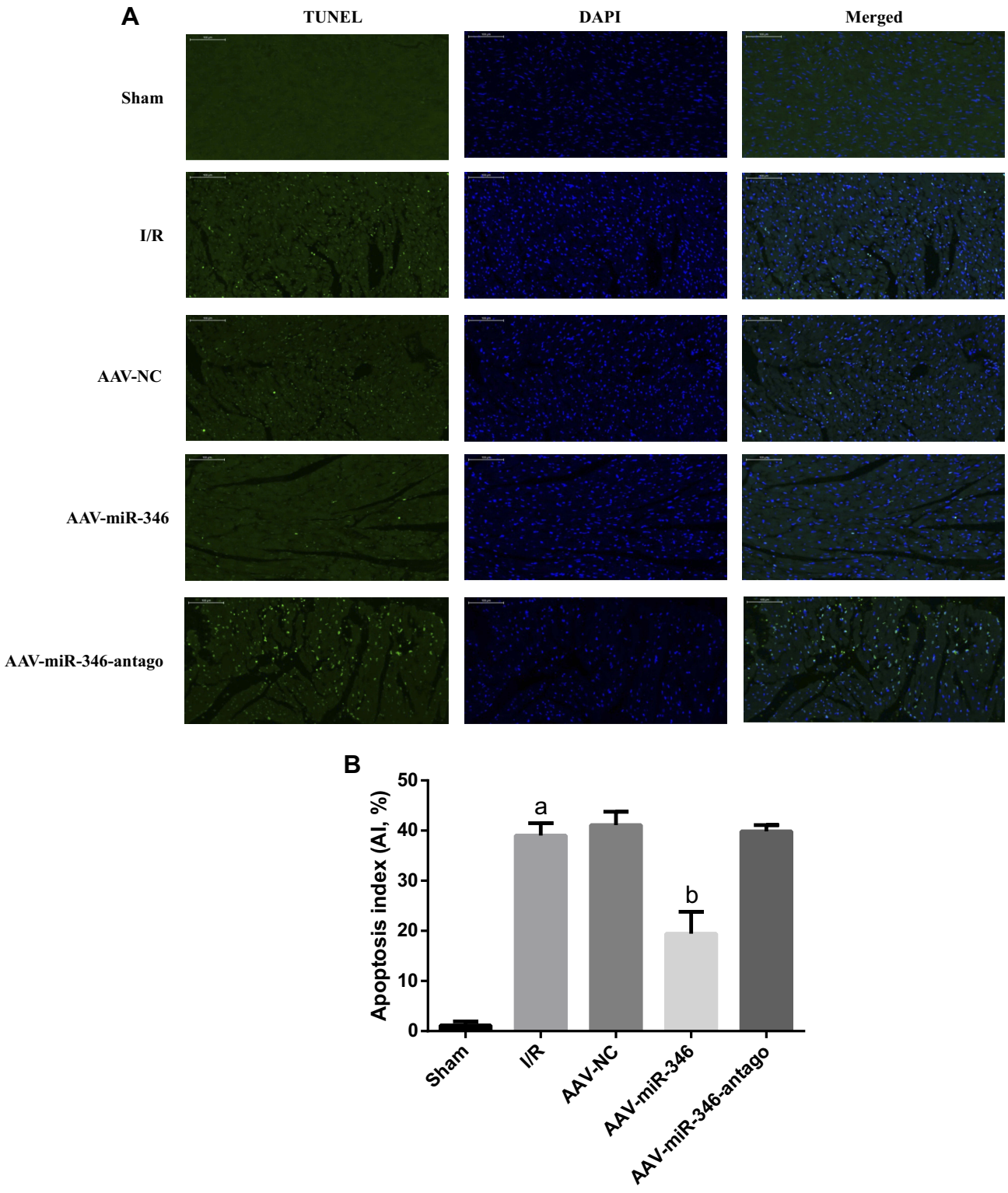

Figure 6 Over-expression of miR-346 inhibited myocardial apoptosis. (**A**) TUNEL staining for myocardial tissues in Sham, I/R, AAV-NC, AAV-miR-346 and AAV-miR-346-antago groups (x200). The green fluorescence represents the TUNEL-positive cardiomyocyte nucleus, and the blue fluorescence represents the total cardiomyocyte nucleus. (**B**) The apoptosis index of each group. Note that $^{a}P < 0.05$ against the Sham group. $^{b}P < 0.05$ against the I/R or AAV-NC group.

displayed in the heat-map, and among them, the expression of 15 miRNAs was significantly downregulated in I/R tissues, miR-346 is one of them. Subsequently, bioinformatic website TargetScan (http://www.targetscan.org/) was utilized to predict the putative downstream effectors of miR-346.

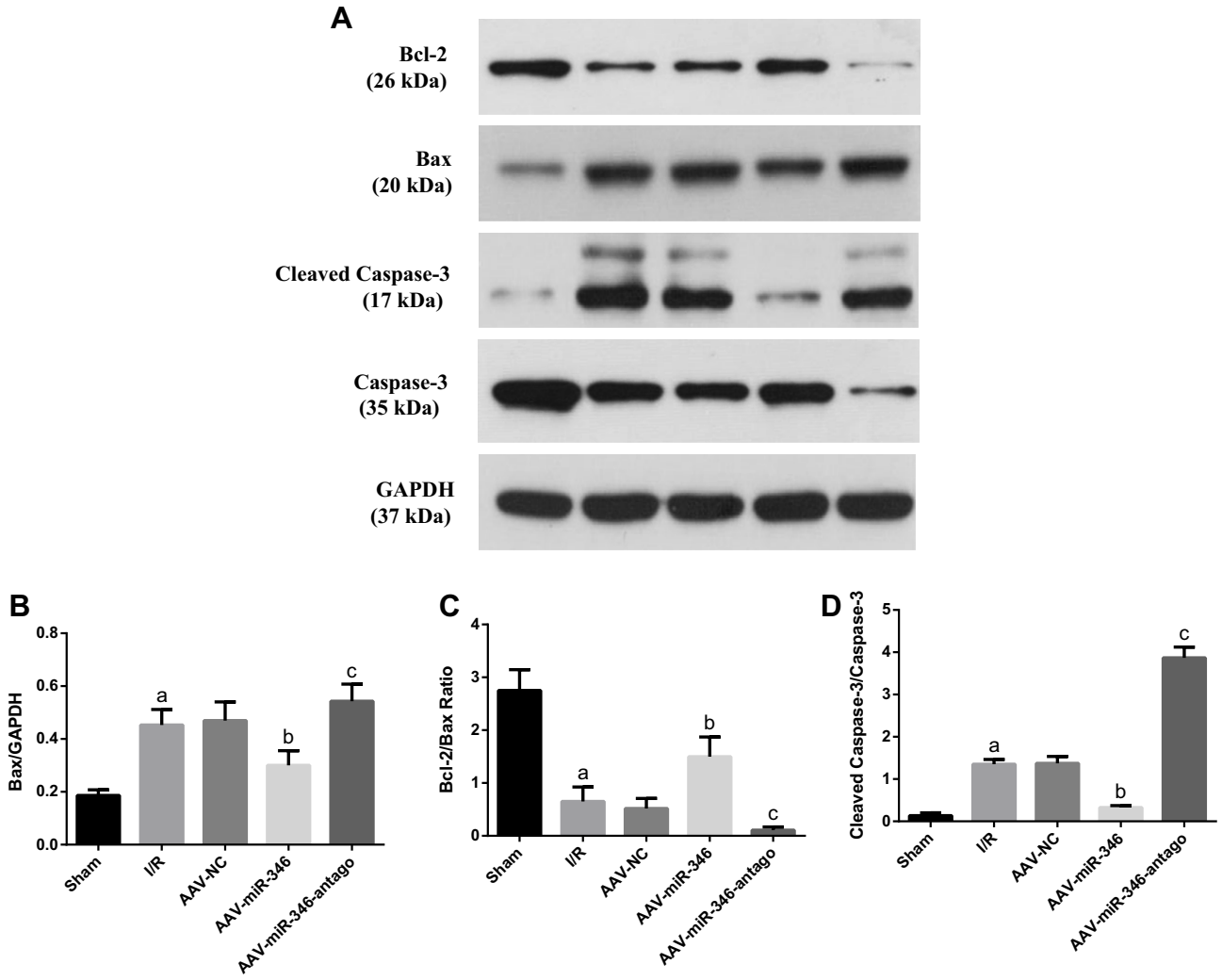

Figure 7 miR-346 inhibited myocardial cell apoptosis mediated by Bax gene. (**A**) Western blotting was used to detect the expression levels of apoptosis-related proteins in Sham, I/R, AAV-NC, AAV-miR-346 and AAV-miR-346-antago groups and quantitative analyses (**B**–**D**). Note that $^{a}P < 0.05$ against the Sham group. $^{b}P < 0.05$ against the I/R or AAV-NC group. $^{c}P < 0.05$ against the I/R group.

Bax, a crucial regulator for cell apoptosis,[49–52] was screened to be a potential target gene of miR-346 with a binding site of miR-346 in its 3′UTR. To identify this prediction, the direct interaction between miR-346 and Bax was confirmed by the luciferase reporter assay. Moreover, overexpression of miR-346 sufficiently evidenced that miR-346 could narrow the infarct size and inhibited the apoptosis. Finally, we authenticated that miR-346 suppressed the apoptosis mainly mediated by Bax.

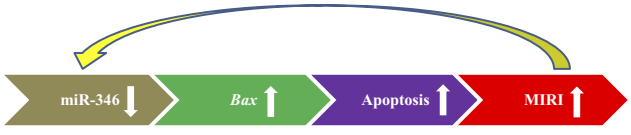

Figure 8 The molecular mechanism diagram showed that miR-346 played an important role in cardiomyocyte apoptosis and the occurrence of MIRI through targeted Bax.

Conclusion

Our findings showed that the exact function of miR-346 during MIRI. Over-expression of miR-346 could sufficiently protect hearts against MIRI. Thus, the miR-346/Bax pathway might be considered as a novel molecular mechanism and therapeutic target to protect against MIRI, as summarized schematically in Figure 8.

Ethics Approval

All protocols and agreements dealing with the experiments were approved by the Ethic Commission of Experimental Animals, Guangxi Medical University.

Acknowledgments

This work was supported by Natural Science Foundation of Guangxi (nos. 2018GXNSFAA294096, 2018GXNSFDA281039); Guilin Medical College The Young and Middle-aged Staff Research Capacity Improvement Project (no. 2018glmcy048); and The Project for Improving the Basic Ability of Young and Middle-aged Teachers in Guangxi Universities (no. 2019KY0532).

Disclosure

The authors report no conflicts of interest in this work.

References

1. Zhai C, Qian Q, Tang G, et al. MicroRNA-206 protects against myocardial ischaemia-reperfusion injury in rats by targeting Gadd45beta. *Mol Cells*. 2017;40(12):916–924. doi:10.14348/molcells.2017.0164
2. Thind GS, Agrawal PR, Hirsh B, et al. Mechanisms of myocardial ischemia-reperfusion injury and the cytoprotective role of minocycline: scope and limitations. *Future Cardiol*. 2015;11(1):61–76. doi:10.2217/fca.14.76
3. He B, Xiao J, Ren AJ, et al. Role of miR-1 and miR-133a in myocardial ischemic postconditioning. *J Biomed Sci*. 2011;18:22. doi:10.1186/1423-0127-18-22
4. Eltzschig HK, Eckle T. Ischemia and reperfusion–from mechanism to translation. *Nat Med*. 2011;17(11):1391–1401. doi:10.1038/nm.2507
5. Yang J, Fan Z, Yang J, Ding J, Yang C, Chen L. microRNA-22 attenuates myocardial ischemia-reperfusion injury via an anti-inflammatory mechanism in rats. *Exp Ther Med*. 2016;12(5):3249–3255. doi:10.3892/etm.2016.3777
6. Botker HE, Hausenloy D, Andreadou I, et al. Practical guidelines for rigor and reproducibility in preclinical and clinical studies on cardioprotection. *Basic Res Cardiol*. 2018;113(5):39.
7. Diaz I, Calderon-Sanchez E, Toro RD, et al. miR-125a, miR-139 and miR-324 contribute to Urocortin protection against myocardial ischemia-reperfusion injury. *Sci Rep*. 2017;7(1):8898. doi:10.1038/s41598-017-09198-x
8. Makhdoumi P, Roohbakhsh A, Karimi G. MicroRNAs regulate mitochondrial apoptotic pathway in myocardial ischemia-reperfusion-injury. *Biomed Pharmacother*. 2016;84:1635–1644. doi:10.1016/j.biopha.2016.10.073
9. Wu HH, Hsiao TY, Chien CT, Lai MK. Ischemic conditioning by short periods of reperfusion attenuates renal ischemia/reperfusion induced apoptosis and autophagy in the rat. *J Biomed Sci*. 2009;16:19. doi:10.1186/1423-0127-16-19
10. Zhou H, Zhu P, Wang J, Zhu H, Ren J, Chen Y. Pathogenesis of cardiac ischemia reperfusion injury is associated with CK2alpha-disturbed mitochondrial homeostasis via suppression of FUNDC1-related mitophagy. *Cell Death Differ*. 2018;25(6):1080–1093. doi:10.1038/s41418-018-0086-7
11. Tian Y, Lv W, Lu C, Zhao X, Zhang C, Song H. LATS2 promotes cardiomyocyte H9C2 cells apoptosis via the Prx3-Mfn2-mitophagy pathways. *J Recept Signal Transduct Res*. 2019;39(5–6):470–478. doi:10.1080/10799893.2019.1701031
12. Zhu H, Fan GC. Role of microRNAs in the reperfused myocardium towards post-infarct remodelling. *Cardiovasc Res*. 2012;94(2):284–292. doi:10.1093/cvr/cvr291
13. Tan H, Qi J, Fan BY, Zhang J, Su FF, Wang HT. MicroRNA-24-3p attenuates myocardial ischemia/reperfusion injury by suppressing RIPK1 expression in mice. *Cell Physiol Biochem*. 2018;51(1):46–62. doi:10.1159/000495161
14. Di YF, Li DC, Shen YQ, et al. MiR-146b protects cardiomyocytes injury in myocardial ischemia/reperfusion by targeting Smad4. *Am J Transl Res*. 2017;9(2):656–663.
15. Bartel DP. MicroRNAs: genomics, biogenesis, mechanism, and function. *Cell*. 2004;116(2):281–297. doi:10.1016/S0092-8674(04)00045-5
16. Doench JG, Sharp PA. Specificity of microRNA target selection in translational repression. *Genes Dev*. 2004;18(5):504–511. doi:10.1101/gad.1184404
17. Zhang B, Pan X, Cobb GP, Anderson TA. microRNAs as oncogenes and tumor suppressors. *Dev Biol*. 2007;302(1):1–12. doi:10.1016/j.ydbio.2006.08.028
18. Shenouda SK, Alahari SK. MicroRNA function in cancer: oncogene or a tumor suppressor? *Cancer Metastasis Rev*. 2009;28(3–4):369–378. doi:10.1007/s10555-009-9188-5
19. Zuo Y, Wang Y, Hu H, Cui W. Atorvastatin protects myocardium against ischemia-reperfusion injury through inhibiting miR-199a-5p. *Cell Physiol Biochem*. 2016;39(3):1021–1030. doi:10.1159/000447809
20. Wang X, Zhang X, Ren XP, et al. MicroRNA-494 targeting both proapoptotic and antiapoptotic proteins protects against ischemia/reperfusion-induced cardiac injury. *Circulation*. 2010;122(13):1308–1318. doi:10.1161/CIRCULATIONAHA.110.964684
21. Zhu Y, Kalbfleisch T, Brennan MD, Li Y. A MicroRNA gene is hosted in an intron of a schizophrenia-susceptibility gene. *Schizophr Res*. 2009;109(1–3):86–89. doi:10.1016/j.schres.2009.01.022
22. Weber F, Teresi RE, Broelsch CE, Frilling A, Eng C. A limited set of human MicroRNA is deregulated in follicular thyroid carcinoma. *J Clin Endocrinol Metab*. 2006;91(9):3584–3591. doi:10.1210/jc.2006-0693
23. Miao X, Wu X, Shi W. MicroRNA-346 regulates neural stem cell proliferation and differentiation by targeting KLF4. *Am J Transl Res*. 2017;9(12):5400–5410.
24. Oskowitz AZ, Lu J, Penfornis P, et al. Human multipotent stromal cells from bone marrow and microRNA: regulation of differentiation and leukemia inhibitory factor expression. *Proc Natl Acad Sci U S A*. 2008;105(47):18372–18377. doi:10.1073/pnas.0809807105
25. Zhu W, Qian J, Ma L, Ma P, Yang F, Shu Y. miR-346 suppresses cell proliferation through SMYD3 dependent approach in hepatocellular carcinoma. *Oncotarget*. 2017;8(39):65218–65229. doi:10.18632/oncotarget.18060
26. Semaan N, Frenzel L, Alsaleh G, et al. miR-346 controls release of TNF-alpha protein and stability of its mRNA in rheumatoid arthritis via tristetraprolin stabilization. *PLoS One*. 2011;6(5):e19827. doi:10.1371/journal.pone.0019827
27. Chen B, Pan W, Lin X, et al. MicroRNA-346 functions as an oncogene in cutaneous squamous cell carcinoma. *Tumour Biol*. 2016;37(2):2765–2771. doi:10.1007/s13277-015-4046-2
28. Yan HL, Li L, Li SJ, Zhang HS, Xu W. miR-346 promotes migration and invasion of nasopharyngeal carcinoma cells via targeting BRMS1. *J Biochem Mol Toxicol*. 2016;30(12):602–607. doi:10.1002/jbt.2016.30.issue-12
29. Zhang WP, Zong QF, Gao Q, et al. Effects of endomorphin-1 postconditioning on myocardial ischemia/reperfusion injury and myocardial cell apoptosis in a rat model. *Mol Med Rep*. 2016;14(4):3992–3998. doi:10.3892/mmr.2016.5695
30. Vaseva AV, Moll UM. The mitochondrial p53 pathway. *Biochim Biophys Acta*. 2009;1787(5):414–420. doi:10.1016/j.bbabio.2008.10.005
31. Zhou M, Liu Z, Zhao Y, et al. MicroRNA-125b confers the resistance of breast cancer cells to paclitaxel through suppression of pro-apoptotic Bcl-2 antagonist killer 1 (Bak1) expression. *J Biol Chem*. 2010;285(28):21496–21507. doi:10.1074/jbc.M109.083337
32. Aneja R, Hake PW, Burroughs TJ, Denenberg AG, Wong HR, Zingarelli B. Epigallocatechin, a green tea polyphenol, attenuates myocardial ischemia reperfusion injury in rats. *Mol Med*. 2004;10(1–6):55–62. doi:10.2119/2004-00032.Aneja

33. Fernandez-Jimenez R, Garcia-Prieto J, Sanchez-Gonzalez J, et al. Pathophysiology underlying the bimodal edema phenomenon after myocardial ischemia/reperfusion. *J Am Coll Cardiol*. 2015;66(7):816–828. doi:10.1016/j.jacc.2015.06.023
34. Heusch G. 25 years of remote ischemic conditioning: from laboratory curiosity to clinical outcome. *Basic Res Cardiol*. 2018;113(3):15. doi:10.1007/s00395-018-0673-2
35. Chang JC, Hu WF, Lee WS, et al. Intermittent hypoxia induces autophagy to protect cardiomyocytes from endoplasmic reticulum stress and apoptosis. *Front Physiol*. 2019;10:995. doi:10.3389/fphys.2019.00995
36. Paradies G, Paradies V, Ruggiero FM, Petrosillo G. Mitochondrial bioenergetics and cardiolipin alterations in myocardial ischemia-reperfusion injury: implications for pharmacological cardioprotection. *Am J Physiol Heart Circ Physiol*. 2018;315(5):H1341–H1352. doi:10.1152/ajpheart.00028.2018
37. Yu L, Zhang W, Huang C, et al. FoxO4 promotes myocardial ischemia-reperfusion injury: the role of oxidative stress-induced apoptosis. *Am J Transl Res*. 2018;10(9):2890–2900.
38. Jin Q, Li R, Hu N, et al. DUSP1 alleviates cardiac ischemia/reperfusion injury by suppressing the Mff-required mitochondrial fission and Bnip3-related mitophagy via the JNK pathways. *Redox Biol*. 2018;14:576–587. doi:10.1016/j.redox.2017.11.004
39. O'Neill LA, Sheedy FJ, McCoy CE. MicroRNAs: the fine-tuners of toll-like receptor signalling. *Nat Rev Immunol*. 2011;11(3):163–175. doi:10.1038/nri2957
40. O'Connell RM, Rao DS, Chaudhuri AA, Baltimore D. Physiological and pathological roles for microRNAs in the immune system. *Nat Rev Immunol*. 2010;10(2):111–122. doi:10.1038/nri2708
41. Long H, Wang X, Chen Y, Wang L, Zhao M, Lu Q. Dysregulation of microRNAs in autoimmune diseases: pathogenesis, biomarkers and potential therapeutic targets. *Cancer Lett*. 2018;428:90–103. doi:10.1016/j.canlet.2018.04.016
42. Evangelatos G, Fragoulis GE, Koulouri V, Lambrou GI. MicroRNAs in rheumatoid arthritis: from pathogenesis to clinical impact. *Autoimmun Rev*. 2019;102391. doi:10.1016/j.autrev.2019.102391
43. Gottlieb RA, Pourpirali S. Lost in translation: miRNAs and mRNAs in ischemic preconditioning and ischemia/reperfusion injury. *J Mol Cell Cardiol*. 2016;95:70–77. doi:10.1016/j.yjmcc.2015.11.011
44. Hu J, Gao C, Wei C, et al. RBFox2-miR-34a-Jph2 axis contributes to cardiac decompensation during heart failure. *Proc Natl Acad Sci U S A*. 2019;116(13):6172–6180. doi:10.1073/pnas.1822176116
45. Li J, Cai SX, He Q, et al. Intravenous miR-144 reduces left ventricular remodeling after myocardial infarction. *Basic Res Cardiol*. 2018;113(5):36. doi:10.1007/s00395-018-0694-x
46. Heallen TR, Kadow ZA, Kim JH, Wang J, Martin JF. Stimulating cardiogenesis as a treatment for heart failure. *Circ Res*. 2019;124(11):1647–1657. doi:10.1161/CIRCRESAHA.118.313573
47. Nattel S. Molecular and cellular mechanisms of atrial fibrosis in atrial fibrillation. *JACC Clin Electrophysiol*. 2017;3(5):425–435. doi:10.1016/j.jacep.2017.03.002
48. Chinchilla A, Daimi H, Lozano-Velasco E, et al. PITX2 insufficiency leads to atrial electrical and structural remodeling linked to arrhythmogenesis. *Circ Cardiovasc Genet*. 2011;4(3):269–279. doi:10.1161/CIRCGENETICS.110.958116
49. Huang K, O'Neill KL, Li J, et al. BH3-only proteins target BCL-xL/MCL-1, not BAX/BAK, to initiate apoptosis. *Cell Res*. 2019;29:942–952. doi:10.1038/s41422-019-0231-y
50. Matarrese P, Tieri P, Anticoli S, et al. X-chromosome-linked miR548am-5p is a key regulator of sex disparity in the susceptibility to mitochondria-mediated apoptosis. *Cell Death Dis*. 2019;10(9):673. doi:10.1038/s41419-019-1888-3
51. Jezek J, Chang KT, Joshi AM, Strich R. Mitochondrial translocation of cyclin C stimulates intrinsic apoptosis through Bax recruitment. *EMBO Rep*. 2019;20(9):e47425. doi:10.15252/embr.201847425
52. Ma G, Liu Y. NURR1 inhibition reduces hypoxia-mediated cardiomyocyte necrosis via blocking Mst1-JNK-mPTP pathway. *J Recept Signal Transduct Res*. 2019;39(4):350–358. doi:10.1080/10799893.2019.1690514